Acta Neuropathol (2009) 117:283–291
DOI 10.1007/s00401-008-0472-1

ORIGINAL PAPER

"Necklace" fibers, a new histological marker of late-onset *MTM1*-related centronuclear myopathy

Jorge A. Bevilacqua · Marc Bitoun · Valérie Biancalana · Anders Oldfors · Gisela Stoltenburg · Kristl G. Claeys · Emmanuelle Lacène · Guy Brochier · Linda Manéré · Pascal Laforêt · Bruno Eymard · Pascale Guicheney · Michel Fardeau · Norma Beatriz Romero

Received: 19 November 2008 / Revised: 2 December 2008 / Accepted: 3 December 2008 / Published online: 16 December 2008

Abstract Mutations in the gene encoding the phosphoinositide phosphatase myotubularin 1 protein (*MTM1*) are usually associated with severe neonatal X-linked myotubular myopathy (XLMTM). However, mutations in *MTM1* have also been recognized as the underlying cause of "atypical" forms of XLMTM in newborn boys, female infants, female manifesting carriers and adult men. We reviewed systematically the biopsies of a cohort of patients with an unclassified form of centronuclear myopathy (CNM) and identified four patients presenting a peculiar histological alteration in some muscle fibers that resembled a necklace ("necklace fibers"). We analyzed further the clinical and morphological features and performed a screening of the genes involved in CNM. Muscle biopsies in all four patients demonstrated 4–20% of fibers with internalized nuclei aligned in a basophilic ring (necklace) at 3 μm beneath the sarcolemma. Ultrastructurally, such necklaces consisted of myofibrils of smaller diameter, in oblique orientation, surrounded by mitochondria, sarcoplasmic reticulum and glycogen granules. In the four patients (three women and one man), myopathy developed in early childhood but was slowly progressive. All had mutations in the MTM1 gene. Two mutations have previously been reported (p.E404K and p.R241Q), while two are novel; a c.205_206delinsAACT frameshift change in exon 4 and a c.1234A>G mutation in exon 11 leading to an abnormal splicing and the deletion of nine amino acids in the catalytic domain of MTM1. Necklace fibers were seen neither in

Electronic supplementary material The online version of this article (doi:10.1007/s00401-008-0472-1) contains supplementary material, which is available to authorized users.

J. A. Bevilacqua · M. Bitoun · P. Laforêt · B. Eymard · P. Guicheney · N. B. Romero
INSERM, U582, Institut de Myologie,
Groupe Hospitalier Pitié-Salpêtrière, 75013 Paris, France

J. A. Bevilacqua · G. Stoltenburg · K. G. Claeys · E. Lacène · G. Brochier · L. Manéré · M. Fardeau · N. B. Romero
Unité de Morphologie Neuromusculaire,
Association Institut de Myologie (AIM),
Groupe Hospitalier Pitié-Salpêtrière, 75013 Paris, France

J. A. Bevilacqua
Departamento de Neurología y Neurocirugía,
HCUCH and Instituto de Ciencias Biomédicas,
Facultad de Medicina, Universidad de Chile, Santiago, Chile

M. Bitoun · P. Laforêt · B. Eymard · P. Guicheney · N. B. Romero
UPMC Univ Paris 06, UMR S582, IFR14, 75013 Paris, France

V. Biancalana
Laboratoire Diagnostic Génétique et EA3949,
Faculté de Médecine, CHRU, Strasbourg, France

A. Oldfors
Department of Pathology,
Sahlgrenska University Hospital, Göteborg, Sweden

K. G. Claeys · E. Lacène · G. Brochier · P. Laforêt · B. Eymard · P. Guicheney · M. Fardeau · N. B. Romero
AP-HP, Groupe Hospitalier Pitié-Salpêtrière,
75013 Paris, France

N. B. Romero (✉)
INSERM U582, Institut de Myologie,
Groupe Hospitalier Pitié-Salpêtrière,
47, Bd de l'Hôpital, 75651 Paris, France
e-mail: nb.romero@institut-myologie.org

DNM2- or *BIN1*-related CNM nor in males with classical XLMTM. The presence of necklace fibers is useful as a marker to direct genetic analysis to *MTM1* in CNM.

Keywords *MTM1* gene · Congenital myopathy · Centronuclear myopathy · *MTM1* mutations

Introduction

Centronuclear myopathies (CNM) are a group of congenital disorders mainly characterized by the presence of central nuclei in the muscle fibers [9, 28]. CNM are divided into three forms, relative to the mode of inheritance. The X-linked recessive myotubular myopathy (XLMTM) is characterized by severe hypotonia and generalized muscle weakness at birth. Most affected boys die during the first year of life from respiratory insufficiency. XLMTM is caused by mutations in the MTM1 gene encoding the phosphoinositide phosphatase myotubularin 1 (MTM1) [21]. Mutations in MTM1 have also been recognized as the underlying cause of atypical forms of XLMTM in newborn boys [7], female infants [17, 30] and adult men and women [1, 13, 14, 16, 27, 32, 33]. The second form is the autosomal dominant CNM usually caused by mutations in the dynamin 2 (DNM2) gene. DNM2 mutations have been associated with a wide clinical spectrum from severe neonatal to milder late-onset CNM including familial or sporadic cases [2–4]. The third form of CNM is an autosomal recessive form (severe neonatal or early-childhood type), which is due to mutations in the BIN1 gene encoding amphiphysin 2 [25].

Here, we report a group of four patients with CNM, including three women and one man, who share a distinctive histological feature, not previously reported in the literature, which we name "necklace fibers." Screening for mutations in the genes known to be associated with CNM (*MTM1*, *DNM2*, *BIN1*) and a candidate gene (*PTPLA*) led to the identification of *MTM1* mutations in the four patients. Our data suggest that the presence of necklace fibers may be a useful marker for late-onset *MTM1*-related myopathy.

Patients and methods

Selection of patients and clinical phenotype studies

In 24 patients diagnosed with CNM by clinical and morphological criteria, we identified a group of four patients with a distinctive muscle biopsy feature: necklace fibers (see "Results"). Patients 1 and 4 were from France, Patient 2 from Portugal and Patient 3 from Sweden. The clinical features of the four patients were retrospectively reviewed. For each of them, the following data were considered: age, sex, age of walking, distribution of weakness, degree of functional impairment according to the Walton Scale at last visit [11], presence of ptosis and extra ocular muscular impairment, cardiac and respiratory functions, orthopedic abnormalities and serum creatine kinase (CK) levels. Computer tomography (CT) and/or magnetic resonance imaging (MRI) were evaluated for Patients 1, 2 and 4. Imaging studies included standard scans at hip, thigh and mid-leg levels.

Morphological studies

Muscle biopsies in Patient 1 were performed at 29 and 43 years of age. In Patients 2–4, muscle biopsies were performed at the ages of 26, 13 and 35 years, respectively. All the biopsies were obtained from the deltoid muscle. Histological analysis of the muscle was performed using staining with hematoxylin and eosin (H&E), Gomori trichrome (GT) and periodic acid-Schiff (PAS) reagent, and histochemical reactions for nicotinamide adenosine dinucleotide–tetrazolium reductase (NADH-TR), myosin adenosine triphosphatase (ATPase) preincubated at pH 9.4, 4.6, 4.3 and cytochrome c oxidase (COX).

The number of fibers with nuclear centralization (i.e., myonuclei in the geometric center of the fiber) and with nuclear internalization (i.e., myonuclei underneath the sarcolemma anywhere within the cytoplasm) were assessed in H&E-stained sections and the number of necklace fibers was assessed in NADH-TR-stained sections. Digital photographs of each biopsy were obtained with a Zeiss AxioCam HRc attached to a Zeiss Axioplan Bright Field Microscope and processed with the AxioVision 4.4 software (Zeiss, Germany). A minimum of 200 adjacent muscle fibers were investigated with each histological technique. The number of necklace fibers was manually counted in four different low power field areas (10×, total numbers of investigated muscle fibers were between 220 and 360 in each specimen). The diameters of all necklace fibers and a minimum of 120 necklace-free fibers were measured manually on the digital pictures of each biopsy using ImageJ 1.40g®, NIH, USA.

Immunohistochemical studies were performed in Patients 1–3. Primary antibodies directed against human desmin (Dako-Desmin, D33, 1:1,000 Dako, Carpinteria, USA); human αB-crystallin (NLC-ABCrys 1:50, Novocastra, Newcastle, UK); human myotilin (NLC-myotilin 1:50, Novocastra); human caveolin 3 [mouse monoclonal 1:500, Affinity Bio Reagents (ABR), Golden, USA] and myosin heavy chain (mouse monoclonal anti-MyHC slow; 1:50, Novocastra) were used. A mixture of antirabbit and antimouse secondary antibodies was incubated according to the standard Ventana System®. Immunoreactivity was visualized by the peroxidase-3′,3′-diaminobenzidine (DAB) method.

Immunofluorescence analyses were performed using antibodies directed against the sarcoplasmic reticulum proteins SERCA1 and SERCA2 (mouse monoclonal NLC-SERCA1 and NLC-SERCA2, 1:200, Novocastra), calsequestrin (mouse monoclonal anti-Calsq 1:500, ABR), ryanodine receptor (mouse monoclonal anti-RYR1, 1:100, ABR), triadin N-terminal domain (TNter, 1:20) [23] and against dihydropyridine receptor-alpha1 subunit (anti-DHPRα1 s, mouse monoclonal, 1:300, ABCAM, Cambridge, UK). Secondary antibodies were goat antimouse-Alexa fluor 488 (Invitrogen, 1:300) for SERCA1 and SERCA2 and CY3 mouse anti-rabbit IgG (Jackson Immuno Research, USA) for the others. A set of control slides was prepared with omission of the primary antibodies. There was no frozen muscle available for inmunohistochemical studies for Patient 4.

Electron microscopy studies were performed in all patients. Muscle specimens were fixed with glutaraldehyde (2.5%, pH 7.4), postfixed with osmium tetroxide (2%), dehydrated and embedded in resin (EMBed-812, Electron Microscopy Sciences, USA). Ultrathin sections were stained with uranyl acetate and lead citrate. The grids were observed using a Philips CM120 electron microscope (80 kV; Philips Electronics NV, Eindhoven, The Netherlands) and were photodocumented using a Morada camera (Soft Imaging System, France).

Genetic analysis

Each patient gave informed consent for the genetic analysis. DNA was extracted from blood samples by standard methods. Exons and intron–exon boundaries of *DNM2*, *BIN1*, *PTPLA* and *MTM1* were analyzed in patients as previously described [1, 4, 19, 22, 25]. Primer sequences and PCR conditions are available on request.

Results

Clinical studies

All four patients were sporadic cases (Table 1). There was neither previous family history of neuromuscular disease nor consanguinity. In all patients, the onset of the muscle involvement was in early childhood. All four patients began walking after 18 months and had delayed motor milestones, poor performance in gymnastics or difficult running and jumping. They presented for medical attention at the age of 10 years (Patient 3) or around the age of 20 years (Patients 1, 2 and 4). Weakness was initially mainly in the proximal lower limbs, spreading later to the distal lower limbs and upper limbs. Muscle power at the shoulder girdle was preserved at onset in all patients, but moderate weakness (MRC grade 3+ to 4) developed later. Neck flexion weakness was present in Patients 1, 2 and 4, and abdominal muscle weakness was prominent in Patients 1 and 2 after the age of 30 years. Contractures were present in all patients. Patient 1 underwent a right Achilles' tenotomy at the age of 10 years, and at 30 years of age, she developed severe contractures of masseters and masticators. Patient 2 had mild finger flexor and bilateral Achilles' tendon contractures. Patient 3 had a slight kypho-scoliosis and talipes cavus. In Patient 4, contractures affecting the neck flexors and masseters developed at 27 years. In this patient, there was ophthalmoparesis for upward gaze.

The four patients had a slowly progressive muscle weakness. At the ages of 47, 32, 17 and 49 years, their levels of disability on the Walton scale were IV, III, II and I, respectively (i.e., Grade IV: the patient walks without assistance but is unable to climb stairs) [11]. Their cardiac function was normal. Patient 1 had a restricted vital capacity (VC) of 83% after the third decade of life, associated with the development of morbid obesity. Patient 3 had a VC of 64% at the age of 13 years. For Patients 2 and 4, VC was within the normal range. CK values were slightly increased in Patients 1, 2 and 4 (184, 395 and 274 U/l, respectively, reference value 160 U/l) and normal for Patient 3 (60 U/l).

CT imaging of Patients 1, 2 and 4 and MRI imaging of Patient 2 showed that the most severe changes occurred in the posterior compartment of the thigh (Fig. 1). The biceps femoris and the semimembranosus and to a lesser extent the semitendinosus were consistently affected at the onset. The adductor magnus was also affected, while adductor longus, sartorius and gracilis were relatively unimpaired. In the anterior compartment of the thigh, signal abnormalities in the vastus intermedius and medialis muscles contrasted with relatively normal appearances in rectus femoris and vastus lateralis. In the lower legs, the soleus was always the most affected muscle and showed moderate to severe changes in the three studied patients. The medial and lateral gastrocnemii, as well as the muscles of the anterior compartment of the leg, were comparatively less involved or unaffected. In the pelvic girdle, moderate to severe abnormalities were observed in the gluteus minimus, medius and maximus. Patients 1 and 4 had asymmetric calves, both having atrophy on the right calf and pseudo-hypertrophy on the left one (Fig. 1). Patient 2 had bilateral calf pseudohypertrophy.

Morphological studies

Marked fiber size variability and predominance of Type I fibers were observed in all patients. Small type I and type II fibers were observed in all patients. Increases in endomysial connective tissue and adipose replacement were present in Patients 1 and 2, but not in the two other patients. Necrosis

Table 1 Summary of clinical and molecular data

Patients	Age years (clinical onset/ current)	Previous family history	Clinical features	Asymmetry	CK** (IU/l)	MTM1 mutation
Patient 1	<3/55	No	Frequent falls, difficulties in running and climbing stairs Muscle testing = Hip M2+/5; Knee M3/5; Ankle Flexors 4/5; Extensors 2/5; Shoulder Girdle M2+/5; Elbow M3/5; Wrist Flexors 4/5; Extensors 3/5; Axial 3/5 Masseters, Achillean contractures	Yes ++; Calf right < left	181	Exon 4; c..205_206delinsAACT (p.R69NfsX5)
Patient 2	<3/32	No	Difficulties in running and climbing stairs Muscle testing = Hip 3/5; Knee Flexors 4/5; Extensors 4/5; Ankle Flexors 4/5; Extensors 3/5; Shoulder Girdle 3/5; Elbow 3/5; Wrist Flexors 4/5; Extensors 3/5; Axial 2+/5 Achillean, finger flexors contractures. Right Babinski's sign	Yes +; Calf right < left	274	Exon 12; c.1262G>A (p.R421Q)
Patient 3	<3/17	No	Delayed motor milestones, difficulties in running Muscle testing = Global 4/5 Gower's sign Kypho-scoliosis, talipes cavus	Yes ++, Left arm and right leg weaker	60	Exon 11; c.1234A>G (p.I412_S420del)
Patient 4	<2/55*	No	Delayed motor milestones Muscle testing = Global 4+/5; Neck 3/5 Ophthlamoplegia, masseters and SCM contractures	Yes +++; Calf right < left	395	Exon.11; c.1206G>A (p.E404K)

Testing graded according to MRC scale. Serum creatine kinase (CK): normal reference value 160 U/l

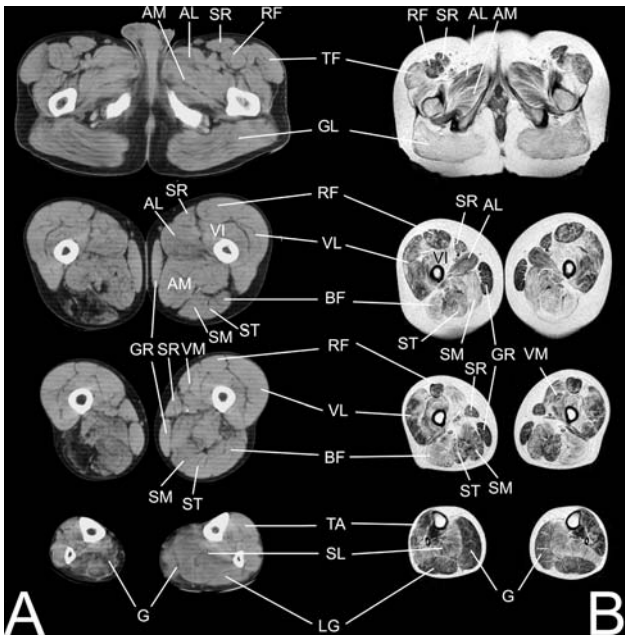

Fig. 1 CT and MRI lower limb imaging of two representative patients. Patient 4 CT scan (**a**), taken at 49 years of age. Asymmetry of calves and selective alteration of right biceps femoris and posterior leg muscles. Patient 2 MRI (**b**), taken at 32 years of age. Marked deterioration of gluteus (*GL*); posterior thigh muscles, vastus intermedius (*VI*) and lateralis (*VL*). Rectus femoris (*RF*), sartorious (*ST*), gracilis (*GR*) and adductor longus (*AL*) muscles were relatively unimpaired. In the leg, the soleus (*SL*) was consistently affected, while gastrocnemius/ gastrocnemii (*GM*) and anterior leg compartment muscles (*TA*) were less affected or unaffected

and regeneration were not observed. On average, 22% of muscle fibers had either central or internalized nuclei. The percentage of fibers with nuclear centralization (mean 5.8%) was consistently lower than that for nuclear internalization (mean 16.2%). In Patient 1, nuclear centralization, nuclear internalization and proportion of Type I fibers were higher in the second biopsy as compared to the first biopsy (Table 2).

With H&E staining, some small fibers showed, underneath the sarcolemma, a basophilic ring or "necklace" that followed the contour of the cell. Fibers with this alteration were hence named "necklace fibers." They frequently assumed a roughly triangular or square shape with rounded corners, and most of the nuclei were in alignment with the necklace and usually located at the corner of the necklace fibers (Figs. 2, 3 and 4). The basophilic necklaces were clearly visible with H&E, GT, PAS and oxidative techniques, but not with myofibrillar ATPase stains. Biopsy immunohistochemistry for Patients 1–3 showed that necklaces were positive for SERCA1 and 2 antibodies (Fig. 3), but not for RYR1, triadin, DHPRα1s and caveolin. Necklaces were also positive for αB-crystallin and desmin. In all three patients, necklace-free fibers stained normally for all antibodies (Fig. 3). The percentage of necklace fibers accounted for 4–20% of all fibers (Table 2). The number of necklace fibers increased in Patient 1 between the first and second biopsy (Table 2). Interestingly, retrospective analysis of a family affected by XLMTM previously reported

Table 2 Summary of morphological parameters of deltoid muscle biopsies with necklace fibers

Patient number	Sex, age Bx (years)	% necklace fibers	% NC	% NI	% NC + NI	% Type I	Necklace fibers main fiber diameter in μm (±SD)	Necklace-free fibers main fiber diameter in μm (±SD)
1[a]								
First	F, 29	4.4	3.1	17.3	20.4	52.0	28.7 (8.4)	75.4 (23.2)
Second	F, 43	8.4	10.0	30.3	40.3	77.3	32.5 (9.5)	72.8 (22.0)
2	F, 26	19.8	8.2	19.8	28.0	99.2	31.8 (8.1)	74.3 (18.2)
3	F, 13	9.1	4.5	8.9	13.4	81.3	29.5 (5.6)	79.3 (60.5)
4	M, 35	5.5	3.0	5.6	8.6	63.2	33.5 (7.8)	77.5 (21.3)

All necklace fibers have internalized nuclei

% NI = percentage of fibers with nuclear internalization; % NC = percentage of fibers with nuclear centralization. References: % NI + % NC = sum of both parameters

[a] Patient 1 had two biopsies; note the increase of all altered parameters between the first and the second biopsies

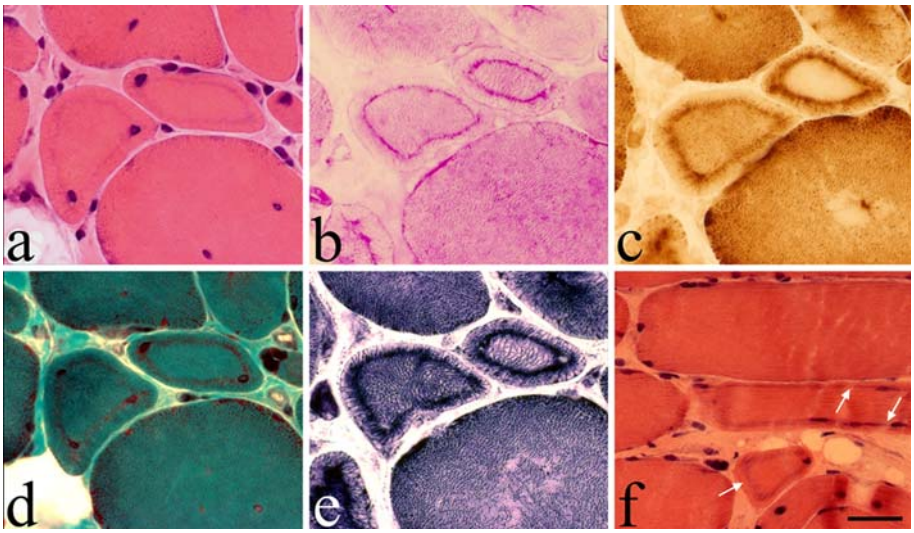

Fig. 2 Light microscopy of necklace fibers with routine staining. Necklace fibers in transverse (**a**–**e**) (Patient 2) and longitudinal (**f**) (Patient 3) sections stained with H&E (**a**, **f**); PAS (**b**); COX (**c**) and NADH-TR (**e**). Necklace fibers are smaller and show a strongly reactive necklace with H&E (**a**, **f**) and GT (**d**), with oxidative techniques (**c**, **e**) and for PAS (**b**), thus indicating the presence of SR, mitochondria and glycogen. We note the presence of myonuclei aligned with the necklace. *Scale bar* **f** 20 μm

[26], and in other two families from our archives, allowed the identification of necklace fibers in the biopsies of obligate female carriers (Supplementary Figure).

Ultrastructural investigation of necklace fibers showed that "necklaces" were consistently located at about 3 μm from the sarcolemma (Fig. 4a, c). The myofibrils within the "necklace" had smaller diameters and oblique orientations compared to myofibrils in other parts of the fibers (Fig. 4c, d). In addition, there was an increase in the density of mitochondria, sarcoplasmic reticulum (SR) and glycogen granules along the "necklaces". Internalized nuclei within the "necklace" region had a normal appearance.

Genetic analysis

No mutation was found in the genes encoding dynamin 2 (*DNM2*), amphiphysin 2 (*BIN1*) and protein tyrosine phosphatase-like member A (*PTPLA*). By sequencing the coding sequence and intron–exon boundaries of the *MTM1* gene, we identified four mutations (Table 1). In Patient 1, a heterozygous deletion–insertion in exon 4 (c.205_206delinsAACT) is predicted to cause a frameshift at Position 69 and a premature stop codon at Position 73 (p.R69NfsX5). Patient 2 harbors a heterozygous missense mutation in exon 12 (c.1262G>A) that changes arginine 421 to glutamine (p.R421Q). In Patient 3, a heterozygous mutation c.1234A>G was identified in exon 11. This change induces the replacement of the wild-type GGATAAGT exonic sequence by GGGTAAGT. This may change the isoleucine at Position 412 to a valine (p.I412 V) or create a new cryptic 5′ donor splice site in intron 11 according to the consensus sequence for the mammalian 5′ splice sites: AGgtragt with r = A or G [31]. For this patient, total RNA was extracted from frozen muscle biopsy and submitted to RT-PCR using sense primer in exon 11 and antisense primer in exon 12. Two amplicons were generated and sequenced: one corresponding to the wild-type sequence and the other to the deletion of the last 27 base pairs of the exon 11, which encode nine

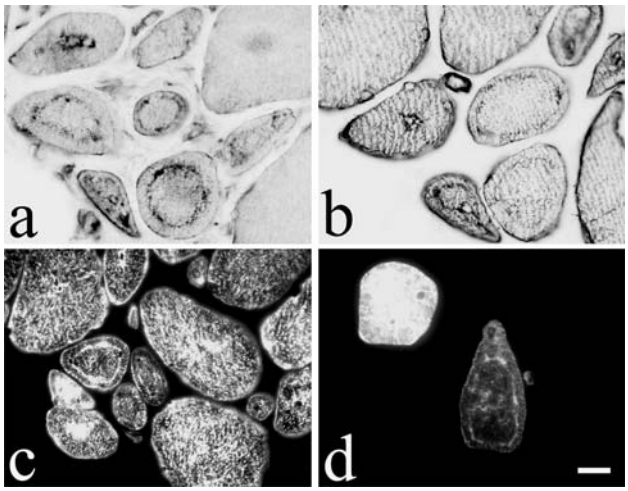

Fig. 3 Immunolabeling of necklace fibers. Transverse muscle sections of biopsies from Patient 3 (**a**–**c**) and from Patient 1 (**d**). Positive labeling of necklaces with anti-desmin (**a**); anti-αB-crystallin (**b**); and anti-SERCA1 or anti-SERCA2 antibodies, in Type I (**c**) and isolated Type II fibers (**d**). The pattern of labelling for all the antibodies was normal in the other fibers of the biopsy. *Scale bar* in **d** 20 μm

amino-acids in the catalytic domain of MTM1, in agreement with the creation of a new splice site (data not shown). This mutation was not found in 200 control subjects. In Patient 4, a missense mutation in exon 11 (c.1210G>A) changes glutamate 404 to lysine (p.E404 K). Mutations in Patients 2 and 4 affect conserved residues within the human MTM1 and orthologues from different species.

Discussion

Centronuclear myopathies (CNM) are a genetically and clinically heterogeneous group of rare neuromuscular disorders in which sporadic cases are frequent. Here, we report the clinical, morphological and genetic characterization of a group of four sporadic patients with CNM identified by the presence of a peculiar morphological marker that we call "necklace fibers." Screening of the genes known to be involved in CNM demonstrated that this group of patients has an atypical, late-onset form of *MTM1*-related CNM.

Molecular analysis demonstrated the presence of *MTM1* mutations in the four patients: three heterozygous mutations in the women and a hemizygous mutation in the man. Among these four mutations, two are novel; a c.205_206delinsAACT in Patient 1 leading to a frameshift and a premature stop codon and a heterozygous missense mutation in Patient 3 (c.1234A>G). This latter mutation creates a new splice site upstream of the exon boundary, as confirmed by cDNA analysis. The two other *MTM1* mutations have already been reported as responsible for XLMTM. The mutation R421Q described in Patient 2 has previously been found in eight male infants with a severe phenotype, and in asymptomatic female carriers [1, 8, 15, 19, 20]. Skewed X inactivation could possibly explain the differential impact of this mutation in symptomatic and asymptomatic women, but this hypothesis could not be analyzed in these patients because material was not available. The mutation in Patient 4 (E404K), the only male of the series, has previously been reported in three male patients between 2 and 68 years of age with mild phenotypes [8, 16].

Clinically, the patients had a mild to moderately severe form of myopathy, with a later onset compared with classical XLMTM myopathy. One prominent feature in three out of four patients (Patients 1, 2 and 4) was the early development of contractures affecting the masticator, neck and limbs muscles. In addition, three out of four patients (Patients 1, 2 and 4) had calf pseudohypertrophy that was asymmetric in the male and in one female patient. Patient 3 had asymmetric left arm and right lower limb weakness. Such asymmetry in *MTM1*-related patients has already been reported in heterozygous manifesting female carriers [13, 14, 27, 32], but not in male patients. In addition, the distribution of the muscle involvement evaluated by CT scan and MRI showed that radiological alterations followed a consistent pattern (Fig. 1), which is different from that seen in DNM2-related myopathy and other congenital myopathies [10, 24].

Radiating sarcoplasmic strands, which is a consistent finding in DNM2-related CNM, myotube-like muscle fibers usually seen in early onset XLMTM, and core-like lesions as seen in CNM associated with RYR1 mutations [18] were not present in our patients. Instead, the four patients exhibited a novel histological feature, i.e., necklace fibers. The morphological aspect of the necklaces, easily visible by histological and histochemical staining in both Type I and Type II fibers is explained by the accumulation of mitochondria, sarcoplasmic reticulum and glycogen granules. Indeed, the density of organelles around the myofibrils in the necklace appeared higher because of the small diameter of the myofibrils, but there no increased number of mitochondria; furthermore, they had normal appearance. Necklace fibers look very different from the classical "ringbinden", which present as a peripheral band constituted by circumferentially oriented fibrils encircling a central region with normally oriented myofibrils; whereas in the "necklace" zone, the myofibrils had oblique orientations and smaller diameters than the myofibrils present in other parts of the fiber, and are located at a constant distance of about 3 μm from the sarcolemma, between two zones of normally sized and oriented myofibrils (Fig. 4). Labelling with anti αB-crystallin and desmin was observed in the necklace region (Fig. 3) in which the size and orientation of the myofibrils were abnormal as was demonstrated by electron microscopy (Fig. 4). As all the muscles biopsies were

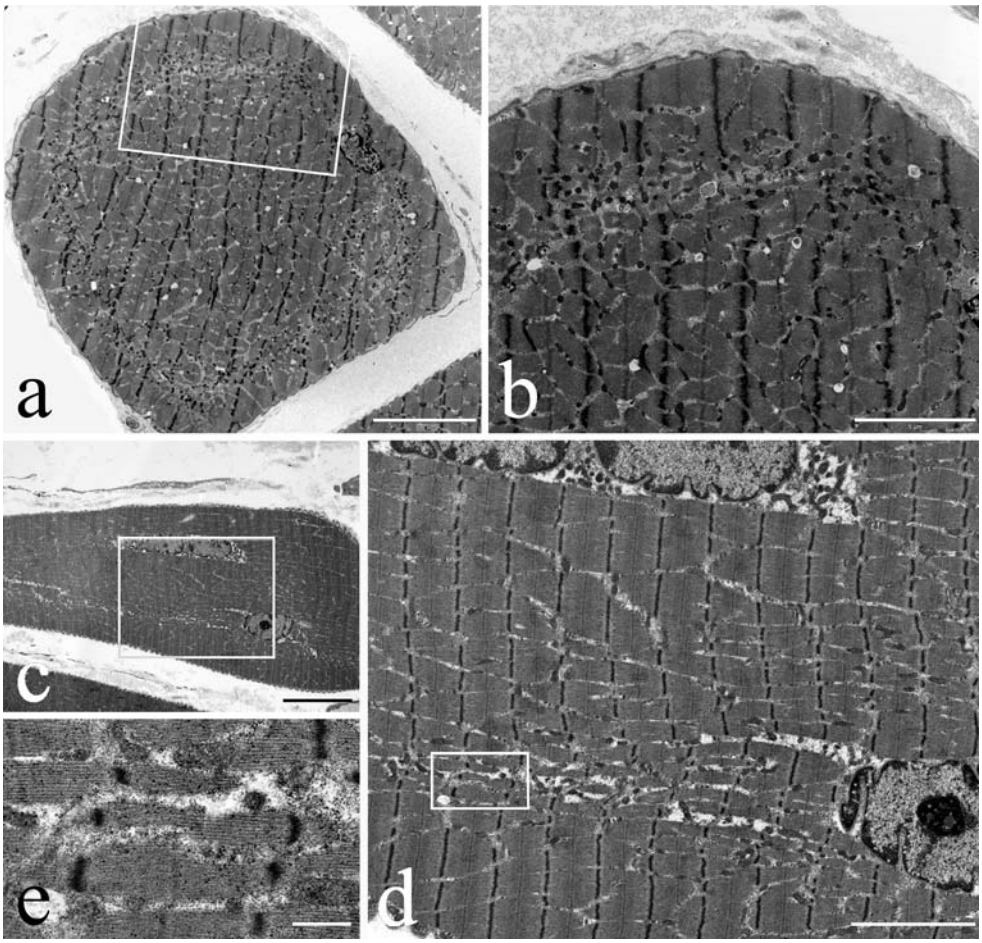

Fig. 4 Ultrastructure of necklace fibers. Atrophic necklace fibers in transverse and longitudinal sections showed two relatively unimpaired and normally structured "areas", one between the necklace and the sarcolemma and the other inside it (**a**–**d**). On longitudinal sections (**c**–**e**), the myofibrils within the necklace showed smaller diameter and an oblique orientation (**d**, **e**). Nuclei aligned with the necklace (**a**, **c**, **d**) and increased number of mitochondria and SR profiles were observed on the necklace (**a**, **b**). Mitochondria, SR profiles and glycogen surrounded the internalized nuclei (**a**, **c**, **d**). *Scale bars* in **a** 10 μm; **b** 5 μm; **c** 20 μm; **d** 7.5 μm; **e** 1 μm

taken from deltoid, this could be a source of sample bias, but we had no muscle biopsies from other regions.

Recently, expression of MTM1-mutants (including the p.R421Q mutation reported here) in cultured cells was shown to result in aggregation of cytoskeletal intermediate filaments by an unknown mechanism [12]. It may be speculated that "necklaces" result from a similar aggregation process of cytoskeletal components leading to alterations in the processes involved in myonuclei and organelle positioning within the fiber. The presence in the necklace of desmin, which is involved in nuclear positioning in skeletal muscle fibers [29], supports this hypothesis.

Among all the previously described biopsies in *MTM1*-related myopathy patients, including the classical severe neonatal XLMTM and atypical late-onset forms affecting adult men or women, the presence of necklace fibers was not reported. Retrospective analysis of muscle biopsies already reported in the literature, especially from patients harboring the two already known mutations p.E404K and p.R421Q, will be necessary to estimate better the proportion of *MTM1*-related myopathy associated with the presence of necklace fibers. In addition to the four patients reported herein, we also identified necklace fibers in the muscle biopsies of two asymptomatic obligate female carriers of two other MTM1 mutations including one family already reported [26]. Similar structural changes have also been reported in the MTM1 knock-out adult mouse [5, 6]. In contrast, we did not identify necklace fibers either in three muscle biopsy specimens from mothers of XLMTM patients with de novo *MTM1* mutations, or from 40 patients with *DNM2*-CNM, or in one patient with *BIN1*-CNM. Overall, these data suggest that the presence of necklace fibers is a marker strongly associated with *MTM1* mutations.

Recent reports have demonstrated that the *MTM1* gene is responsible for a much broader range of phenotypes than

initially appreciated, both in males and females. In cases of clinical diagnostic difficulty in which the mode of inheritance remains uncertain, recognition of necklace fibers in muscle biopsy specimens should be followed by *MTM1* screening irrespective of the patient's age and gender. In conclusion, necklace fibers could become a useful specific histological marker to target molecular screening, in particular for female patients, considering the high risk of having severely affected male infants.

Acknowledgments We are grateful to Nigel Clarke, MD, PhD, for his helpful advice; Michael Walls, PhD, for critical reading of the manuscript; Isabelle Marty, PhD, for providing anti-triadin antibodies; Andrée Rouche, MSc, Svetlana Maugenre, BSc, Bernard Prudhon, BSc, and Nicolas Dondaine, BSc, for expert technical assistance. This work was supported by the Institut National de la Santé et de la Recherche Médicale (INSERM) and the Association Française contre les Myopathies (AFM). J. A. Bevilacqua was supported by the Program Alban; The European Union Program of High Level Scholarships for Latin America (Scholarship No. E04E028343CL); and the Association Institut de Myologie (AIM), France.

Conflict of interest statement The authors have no conflicts of interest.

References

1. Biancalana V, Caron O, Gallati S et al (2003) Characterisation of mutations in 77 patients with X-linked myotubular myopathy, including a family with a very mild phenotype. Hum Genet 112:135–142
2. Bitoun M, Bevilacqua JA, Eymard B, Fardeau M, Guicheney P, Romero NB (2009) An atypical phenotype of centronuclear myopathy due to a novel dynamin 2 mutation. Neurology 72(1)
3. Bitoun M, Bevilacqua JA, Prudhon B et al (2007) Dynamin 2 mutations cause sporadic centronuclear myopathy with neonatal onset. Ann Neurol 62:666–670
4. Bitoun M, Maugenre S, Jeannet P-Y et al (2005) Mutations in dynamin 2 cause dominant centronuclear myopathy. Nat Genet 37:1207–1209
5. Buj-Bello A, Fougerousse F, Schwab Y et al (2008) AAV-mediated intramuscular delivery of myotubularin corrects the myotubular myopathy phenotype in targeted murine muscle and suggests a function in plasma membrane homeostasis. Hum Mol Genet 17:2132–2143
6. Buj-Bello A, Laugel V, Messaddeq N et al (2002) The lipid phosphatase myotubularin is essential for skeletal muscle maintenance but not for myogenesis in mice. Proc Natl Acad Sci USA 9923:15060–15065
7. de Goede CGEL, Kinsley A, Kingston H, Tomlin PI, Hughes MI (2005) Muscle biopsy without centrally located nuclei in a male child with mild X-linked myotubular myopathy. Dev Med Child Neurol 47:835–837
8. de Gouyon BM, Zhao W, Laporte J, Mandel JL, Metzenberg A, Herman GE (1997) Characterization of mutations in the myotubularin gene in twenty six patients with X-linked myotubular myopathy. Hum Mol Genet 6:1499–1504
9. Fardeau M, Tomé F (1994) Congenital myopathies. In: Engel AG, Franzini-Armstrong C (eds) Myology, 2nd edn. McGraw Hill, New York, pp 1500–1505
10. Fischer D, Herasse M, Bitoun M et al (2006) Characterization of the muscle involvement in dynamin 2 related centronuclear myopathy. Brain 129:1463–1469
11. Gardner-Medwin D, Walton JN (1974) The clinical examination of the voluntary muscles. In: Walton JN (ed) Disorders of voluntary muscles. Churchill-Livingstone, Edinburgh, pp 517–560
12. Goryunov D, Nightingale A, Bornfleth L, Leung C, Liem RKH (2008) Multiple disease-linked myotubularin mutations cause NFL assembly defects in cultured cells and disrupt myotubularin dimerization. J Neurochem 104:1536–1552
13. Grogan PM, Tanner SM, Ørstavik KH et al (2005) Myopathy with skeletal asymmetry and hemidiaphragm elevation is caused by myotubularin mutations. Neurology 64:1638–1640
14. Hammans SR, Robinson DO, Moutou C et al (2000) A clinical and genetic study of a manifesting heterozygote with X-linked myotubular myopathy. Neuromuscul Disord 10:133–137
15. Herman GE, Kopacz K, Zhao W, Mills PL, Metzenberg A, Das S (2002) Characterization of mutations in fifty North American patients with X-linked myotubular myopathy. Hum Mutat 192:114–121
16. Hoffjan S, Thiels C, Vorgerd M, Neuen-Jacob E, Epplen J, Kress W (2006) Extreme phenotypic variability in a German family with X-linked myotubular myopathy associated with E404 K mutation in MTM1. Neuromuscul Disord 16:749–753
17. Jungbluth H, Sewry CA, Buj-Bello A et al (2003) Early and severe presentation of X-linked myotubular myopathy in a girl with skewed X-inactivation. Neuromuscul Disord 13:55–59
18. Jungbluth H, Zhou H, Sewry CA et al (2007) Centronuclear myopathy due to a *de novo* dominant mutation in the skeletal muscle ryanodine receptor (RYR1) gene. Neuromuscul Disord 17:338–345
19. Laporte J, Biancalana V, Tanner S, Kress W, Schneider V, Wallgren-Pettersson C (2000) MTM1 mutations in X-linked myotubular myopathy. Hum Mutat 15:393–409
20. Laporte J, Guiraud-Chaumeil C, Vincent MC et al (1997) Mutations in the MTM1 gene implicated in X-linked myotubular myopathy. Hum Mol Genet 6:1505–1511
21. Laporte J, Hu LJ, Kretz C et al (1996) A gene mutated in X-linked myotubular myopathy defines a new putative tyrosine phosphatase family conserved in yeast. Nat Genet 13:175–182
22. Li D, Gonzalez O, Bachinski LL, Roberts R (2000) Human protein tyrosine phosphatase-like gene: expression profile, genomic structure, and mutation analysis in families with ARVD. Gene 256:237–243
23. Marty I, Thevenon D, Scotto C et al (2000) Cloning and characterization of a new isoform of skeletal muscle triadin. J Biol Chem 275:8206–8212
24. Mercuri E, Pichiecchio A, Allsop J, Messina S, Pane M, Muntoni F (2007) Muscle MRI in inherited neuromuscular disorders: past, present, and future. J Magn Reson Imaging 25:433–440
25. Nicot AS, Toussaint A, Tosch V et al (2007) Mutations in amphiphysin 2 BIN1 disrupt interaction with dynamin 2 and cause autosomal recessive centronuclear myopathy. Nat Genet 33:1134–1139
26. Oldfors A, Kyllerman M, Wahlström J, Darnfors C, Henriksson KG (1989) X-linked myotubular myopathy: clinical and pathological findings in a family. Clin Genet 361:5–14
27. Pénisson-Besnier I, Biancalana V, Reynier P, Cossée M, Dubas F (2007) Diagnosis of myotubular myopathy in the oldest known manifesting female carrier: a clinical and genetic study. Neuromuscul Disord 172:180–185
28. Pierson CR, Tomczak K, Agrawal P, Moghadaszadeh B, Beggs AH (2005) X-linked myotubular and centronuclear myopathies. J Neuropathol Exp Neurol 64(7):555–564
29. Ralston E, Lu Z, Biscocho N et al (2006) Blood vessels and desmin control the positioning of nuclei in skeletal muscle fibers. J Cell Physiol 209:874–882
30. Schara U, Kress W, Tücke J, Mortier W (2003) X-linked myotubular myopathy in a female infant caused by a new MTM1 gene mutation. Neurology 60:1363–1365

31. Shapiro MB, Senapathy P (1987) RNA splice junctions of different classes of eukaryotes: sequence statistics and functional implications in gene expression. Nucleic Acids Res 15:7155–7174
32. Sutton IJ, Winer JB, Norman AN, Liechti-Gallati S, MacDonald F (2001) Limb girdle and facial weakness in female carriers of X-linked myotubular myopathy mutations. Neurology 57:900–902
33. Yu S, Manson S, White S et al (2003) X-linked myotubular myopathy in a family with three adult survivors. Clin Genet 64:148–152